# ECOLE NORMALE SUPERIEURE

More icosahedral fulleroids

Olaf DELGADO FRIEDRICHS
Michel DEZA

## Département de Mathématiques et Informatique

# More icosahedral fulleroids

Olaf DELGADO FRIEDRICHS[*]

Michel DEZA

Laboratoire d'Informatique de l'Ecole Normale Supérieure
45 rue d'Ulm 75230 PARIS Cedex 05

Tel : (33)(1) 01 44 32 30 00

Adresse électronique : deza@dmi.ens.fr

[*]Fakultät für Mathematik, Universität Bielefeld,
33501 Bielefeld, Germany

Adresse électronique : delgado@Mathematik.Uni-Bielefeld.DE

# More icosahedral fulleroids

## Olaf Delgado Friedrichs and Michel Deza

ABSTRACT. Generalized fullerenes — or fulleroids — containing faces of degree larger than 6, are beginning to gain some interest in theoretical chemistry. Using the theory of *Delaney symbols*, we construct some relatively small fulleroids with icosahedral symmetries and without hexagons and which are unique with respect to their p-vectors and symmetries. We also obtain several infinite series of icosahedral fulleroids.

## 1. Introduction

Dress and Brinkmann [**DB96**] introduce *Fowler's Phantasmagorical Fulleroids* as the two unique planar polyhedral maps (or tilings of the sphere) with p-vector $(p_5, p_7) = (72, 60)$ and icosahedral symmetry. Their proof that no other such structures exist exemplifies the power and beauty of the method of Delaney symbols. Although for larger structures, the necessary case analysis becomes rather tedious and requires the help of a computer (cf. [**Hus93**]), a number of similar classification results come up even more easily by the same general scheme.

The structures found by Dress and Brinkmann as well as the ones we will describe here can be constructed from certain well-known icosahedral fullerenes using simple subdivision operations. By applying such operations to infinite series of fullerenes, one obtains corresponding infinite series of fulleroids.

We will use the terminology of [**DB96**] plus the following definitions: a *fulleroid* is a tiling of the sphere such that all of its vertices have degree 3 while all of its faces have degree 5 or larger. A $\Gamma$-*fulleroid* is a fulleroid on which the group $\Gamma$ acts as a group of symmetries. In particular, an *I*-fulleroid is one which has the same proper (i.e., orientation preserving) symmetries as the icosahedron. The *p-vector* (c.f. [**Grü67**]) of a tiling is a vector $(p_i)_{i \in \mathbf{N}}$ such that $p_i$ denotes the number of faces of degree $i$ in that tiling.

We will say that a given *I*-fulleroid $F$ is of *type* $(a, b)$ or an *I(a, b)-fulleroid*, if $p_i(F)$ is nonzero if and only if $i \in \{a, b\}$. See [**DG97**] for a more general study of such bifaced polyhedra. Let $a = 5$. The case $b < 5$ is not possible. For $a = b = 5$, the only possible *I*-fulleroid is the dodecahedron. The case $(a, b) = (5, 6)$ is the classical fullerene case. There is a well-known classification result for $I(5, 6)$-fulleroids, i.e. fullerenes of icosahedral symmetry ([**Gol37**] and [**Cox71**]). The smallest possible $I(5, 7)$-fulleroids are described in [**DB96**]. Here, we will look at the smallest $I(5, n)$-fulleroids for some numbers $n > 7$.

We will proceed as follows: in Section 2, we will describe and tabulate the new structures. All *I*-fulleroids known so far can be conveniently described as the

result of regularly "decorating" certain well-known fullerenes. In Section 3, we will describe these decorations and introduce some infinite series of fulleroids which are obtained this way. Most remarkably, we will show that there are infinitely many $I(5,7)$- and $I(5,8)$-fulleroids. Then, in Section 4, we will derive a necessary condition on the p-vectors which implies that five of the new $I$-fulleroids are minimal for their respective values of $n$. Finally, in Section 5, we will apply the method of Delaney-symbols by A. Dress to establish the uniqueness of five of the new fulleroids and the minimality of the one not handled by Section 4.

## 2. Results

For later reference, we will start by describing the four smallest icosahedral fullerenes apart from the dodecahedron. The first one is $C_{60}(I_h)$, the bucky-ball or buckminsterfullerene. The second one is $C_{80}(I_h)$, the 'chamfered' dodecahedron, obtained from the dodecahedron by capping each face with a pentagonal prism, then removing all original edges. The other two are $C_{140}(I)$ and, finally, $C_{180}(I_h)$, the 'leap-frog' of the bucky-ball, obtained from the dual of $C_{60}(I_h)$ by truncating all the vertices. For reference, we show the first three of these well-known fullerenes in Figure 1. We use a simplified version of the conventional naming for fullerenes here, where $C_n(\Gamma)$ stands for a 'carbon molecule' with $n$ atoms (i.e. a three-regular graph with $n$ vertices) and full combinatorial symmetry group $\Gamma$. Although this notation is not generally unique, it will suffice for our purpose.



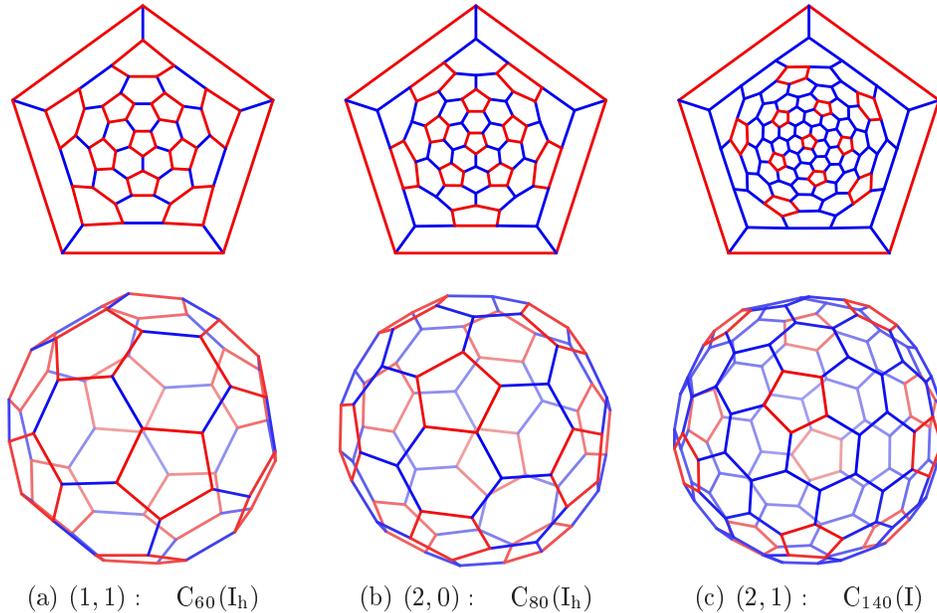(a) $(1,1)$ :  $C_{60}(I_h)$          (b) $(2,0)$ :  $C_{80}(I_h)$          (c) $(2,1)$ :  $C_{140}(I)$

FIGURE 1. The icosahedral fullerenes with parameters $(1,1)$, $(2,0)$ and $(2,1)$

The four polyhedra mentioned above have parameters $(1,1)$, $(2,0)$, $(2,1)$ and $(3,0)$, respectively, as according to Goldberg [Gol37], while the dodecahedron has

parameters $(1, 0)$. These parameters refer to the distance vectors w.r.t. the hexagonal lattice $A_2$ between pairs of closest pentagons. We will sometimes use the notation $G_{p,q}$ for an icosahedral fullerene with Goldberg parameters $(p, q)$.

Dress and Brinkmann show that the two $I(5, 7)$-fulleroids they describe are the only such structures with the (smallest possible) p-vector $(p_5, p_7) = (72, 60)$. We will generalize their result to $I(5, n)$-fulleroids, where $n = 8, 9, 10, 12, 14, 15$.

Note that because of Equation 4.1 below, the numbers $p_a$ and $p_b$ in an $I(a, b)$-fulleroid are linear functions of each other. This further implies that $v$, the number of vertices, is a linear function of any one of them. Therefore, we can use any one of these three quantities to measure the size of an $I(a, b)$-fulleroid. However, for $I(5, n)$-fulleroids, it will turn out to be most convenient to use $p_n$.

Table 1 shows the smallest possible p-vectors for $7 \leq n \leq 20$ according to Lemma 4.3 below. The first four columns of the table show the quantities $n$, $p_5$, $p_n$ and $v$ as defined above. Note that since all graphs described here are 3-regular (each vertex has valency three), the number of edges is simply $e = 3v/2$. The invariants $m_5$, $m_n$, $k_2$, $k_3$ and $k_5$ are described in Section 4. The last three columns, if applicable, give the number (#) of structures with the given p-vector, the numbers of the figures in which they appear and the names by which we will refer to them. These names are of the form $F_{a,b}(\Gamma)$, where $(a, b)$ is the type and $\Gamma$ is the full combinatorial symmetry group of the fulleroid. Note that for $n = 12$, the smallest p-vector which fullfills the condition of the lemma is not realizable. The smallest $I(5, 12)$-fulleroid has as its p-vector the second to smallest one predicted by that condition, which is also shown.

| n | $p_5$ | $p_n$ | v | $m_5$ | $m_n$ | $k_2$ | $k_3$ | $k_5$ | # | Fig. | Name(s) |
|---|-------|-------|---|-------|-------|-------|-------|-------|---|------|---------|
| **7** | **72** | **60** | **260** | **1** | **1** | **3** | **2** | **1** | **2** | **(2)** | $\mathbf{F_{5,7}(I)a}$ |
| | | | | | | | | | | (3) | $\mathbf{F_{5,7}(I)b}$ |
| **8** | **72** | **30** | **200** | **1** | **1** | **4** | **2** | **1** | **1** | **(5)** | $\mathbf{F_{5,8}(I_h)}$ |
| **9** | **72** | **20** | **180** | **1** | **0** | **3** | **3** | **1** | **1** | **(4)** | $\mathbf{F_{5,9}(I_h)}$ |
| **10** | **60** | **12** | **140** | **1** | **0** | **3** | **2** | **2** | **1** | **(6)** | $\mathbf{F_{5,10}(I_h)}$ |
| 11 | 312 | 60 | 740 | 5 | 1 | 3 | 2 | 1 | ? | | |
| 12 | 132 | 20 | 300 | 2 | 0 | 3 | 4 | 1 | − | | |
| **12** | **192** | **30** | **440** | **3** | **0** | **6** | **3** | **1** | **1** | **(8)** | $\mathbf{F_{5,12}(I_h)}$ |
| 13 | 432 | 60 | 980 | 7 | 1 | 3 | 2 | 1 | ? | | |
| **14** | **252** | **30** | **560** | **4** | **0** | **7** | **2** | **1** | **1** | **(9)** | $\mathbf{F_{5,14}(I_h)}$ |
| **15** | **120** | **12** | **260** | **2** | **0** | **3** | **2** | **3** | **1** | **(7)** | $\mathbf{F_{5,15}(I_h)}$ |
| 16 | 312 | 30 | 680 | 5 | 0 | 8 | 2 | 1 | ? | | |
| 17 | 672 | 60 | 1460 | 11 | 1 | 3 | 2 | 1 | ? | | |
| 18 | 252 | 20 | 540 | 4 | 0 | 3 | 6 | 1 | ? | | |
| 19 | 792 | 60 | 1700 | 13 | 1 | 3 | 2 | 1 | ? | | |
| 20 | 180 | 12 | 380 | 3 | 0 | 3 | 2 | 4 | ? | | |

TABLE 1. Potential p-vectors and invariants for certain $I(5, n)$-fulleroids.

Figures 4 to 9 contain Schlegel diagrams and spatial embeddings with about constant edge lengths of the 6 new fulleroids. For reference, we also include pictures of the 2 structures from [**DB96**] as Figures 2 and 3. The coordinates for all of these figures where obtained by the algorithms described in [**Del98**].
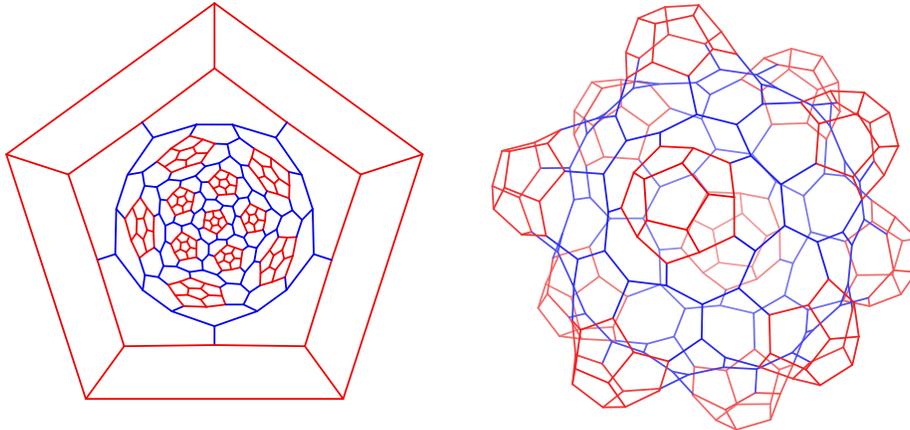
FIGURE 2. $F_{5,7}(I)a = P(C_{140}(I))$; $v = 260$
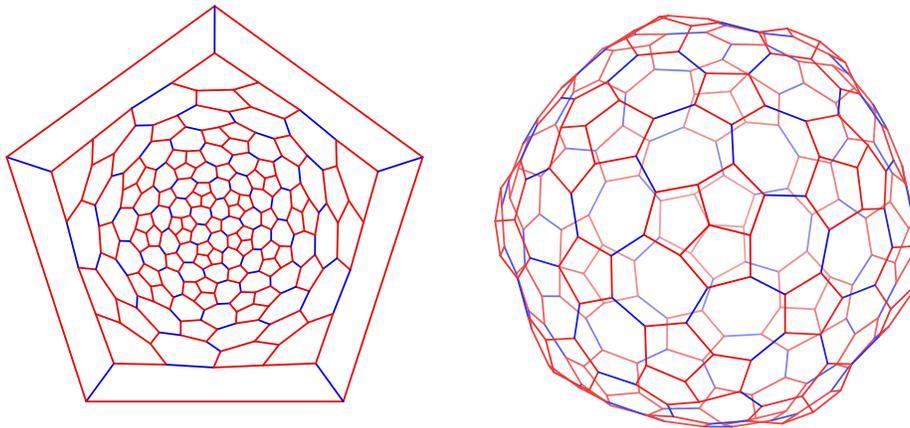


FIGURE 3. $F_{5,7}(I)b = T_1(C_{180}(I_h))$; $v = 260$

## 3. The decoration operations

The six fulleroids shown in the previous section as well as the two described by Brinkmann and Dress have been found by a systematic investigation of *all* possible ways to assemble pentagons and, say, octagons into a structure with the desired properties. This will be explained in more detail in Section 5. However, it turns out that all eight structures can be conveniently described as the results of decorating small icosahedral fullerenes with symmetric patches from the dodecahedron. By applying these decorations to other icosahedral fullerenes, one obtains several infinite series of $I$-fulleroids. The two most interesting of these are an infinite series of $I(5,7)$-fulleroids and a similar series of $I(5,8)$-fulleroids.

We need the following four decoration operations producing pentagons:
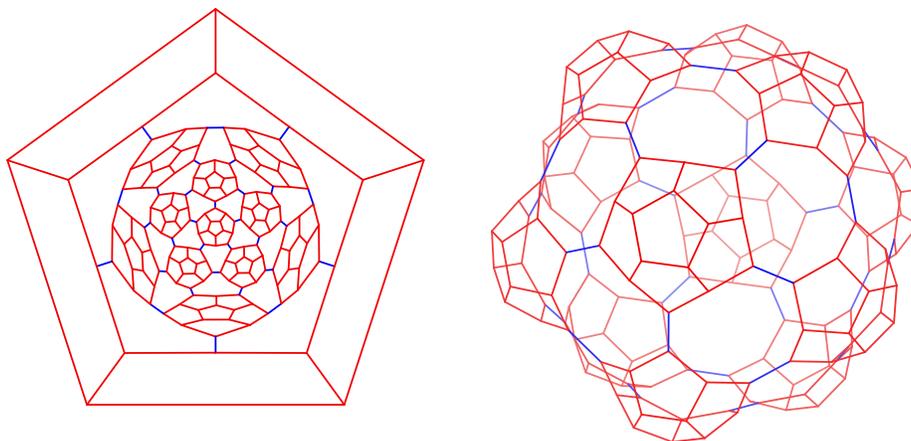
FIGURE 4. $F_{5,9}(I_h) = P(C_{60}(I_h))$; $v = 180$
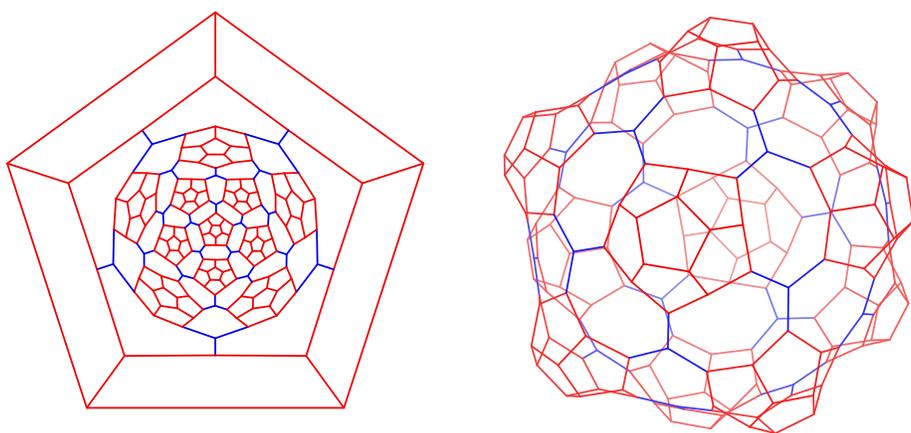


FIGURE 5. $F_{5,8}(I_h) = P(C_{80}(I_h))$; $v = 200$

**Triacon of first order:** Split a hexagon into three pentagons by connecting midpoints of three pairwise nonadjacent sides to the face center.

**Pentacon:** Split a pentagon into five quadrangles by connecting midpoints of all sides to the face center, then truncate the central vertex to obtain six pentagons.

**Triacon of second order:** Split a hexagon into three quadrangles and a hexagon by three new edges parallel to pairwise nonadjacent sides, then apply the triacon of first order to the new hexagon, using midpoints of new edges, to obtain altogether six pentagons.

**Triacon of third order:** Split a triangle into three new triangles and a hexagon by "cutting off" the vertices, then apply the triacon of second order to the hexagon to obtain altogether nine pentagons.
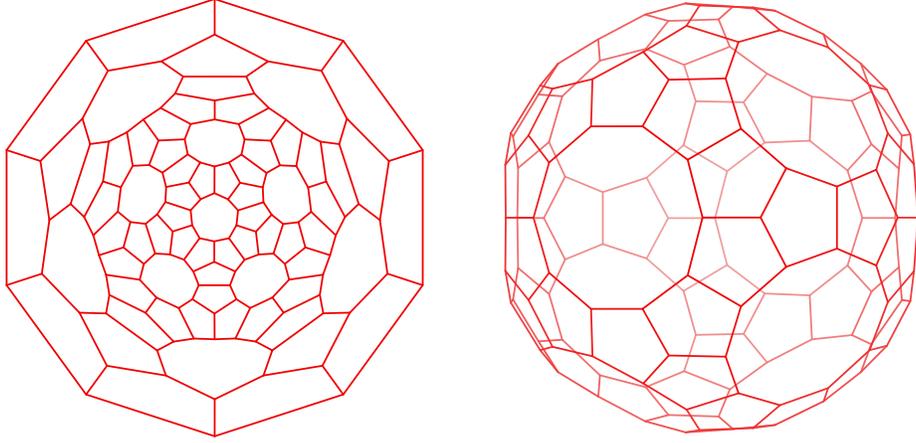
FIGURE 6. $F_{5,10}(I_h) = T_1(C_{60}(I_h))$; $v = 140$
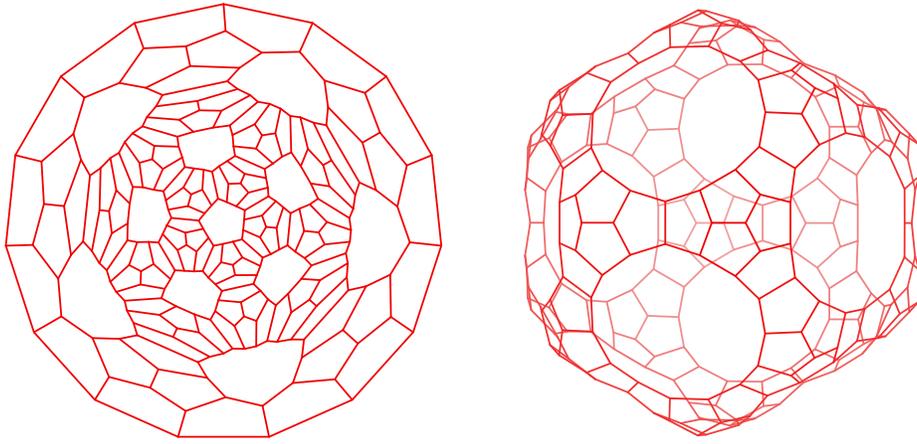


FIGURE 7. $F_{5,15}(I_h) = T_2(C_{60}(I_h))$; $v = 260$

Note that these operations retain the full rotational symmetry of the face they are applied to, but that the first two triacon operations will destroy mirror symmetries in case a mirror plane intersects the decorated hexagon at two opposite vertices.

In Table 2, we summarize the relations between small icosahedral fullerenes and fulleroids in terms of the four decoration operations. For that purpose, we denote the application of the pentacon operation to a complete set of 12 pentagons containing a 5-fold symmetry axis each by the letter $P$. We denote the application of the first two triacon operations to sets of 20 faces containing a 3-fold rotational axis each by $T_1$ and $T_2$, respectively. If for some base structure the 3-fold axes meet vertices, then we denote the operation of truncating all 20 such vertices and applying the triacon of third order to the resulting triangles by $T_3$.
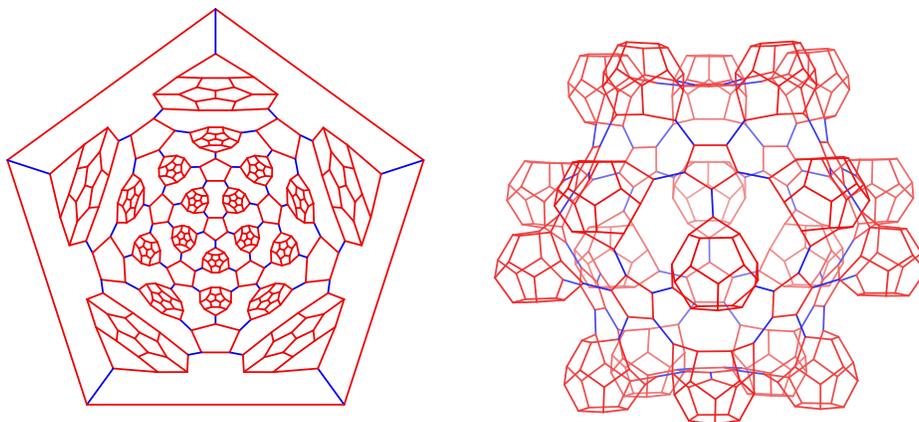
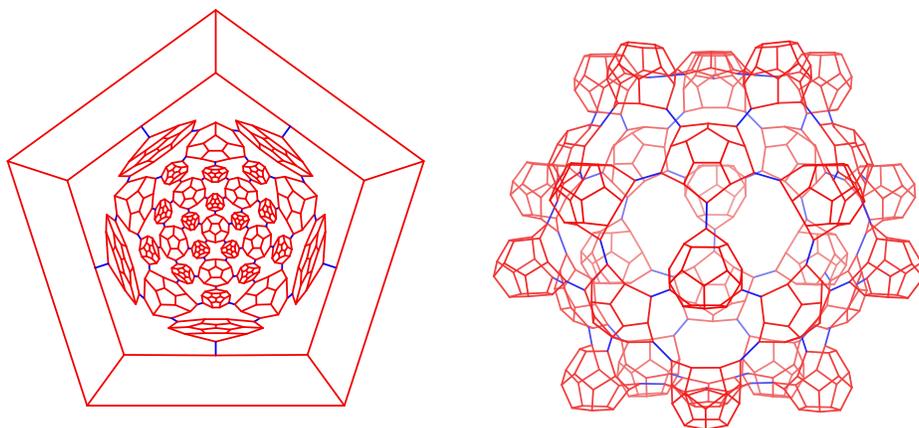FIGURE 8. $F_{5,12}(I_h) = T_3(C_{80}(I_h))$; $v = 440$



FIGURE 9. $F_{5,14}(I_h) = P(F_{5,12}(I_h))$; $v = 560$

$$
\begin{aligned}
F_{5,7}(I)a &= P(C_{140}(I)) \\
F_{5,7}(I)b &= T_1(C_{180}(I_h)) \\
F_{5,8}(I_h) &= P(C_{80}(I_h)) \\
F_{5,9}(I_h) &= P(C_{60}(I_h)) \\
F_{5,10}(I_h) &= T_1(C_{60}(I_h)) \\
F_{5,12}(I_h) &= T_3(C_{80}(I_h)) \\
F_{5,14}(I_h) &= P(F_{5,12}(I_h)) = T_3(F_{5,8}(I_h)) \\
F_{5,15}(I_h) &= T_2(C_{60}(I_h))
\end{aligned}
$$

TABLE 2. Description of fulleroids as decorated fullerenes

Note that the triacon of $C_{180}(I_h)$ has only $I$-symmetry due to the fact that the triacon operations do not always retain mirror symmetries. Also note that $F_{5,14}(I_h)$ is obtained from $C_{80}(I_h)$ by applying both $P$ and $T_3$, in any order.
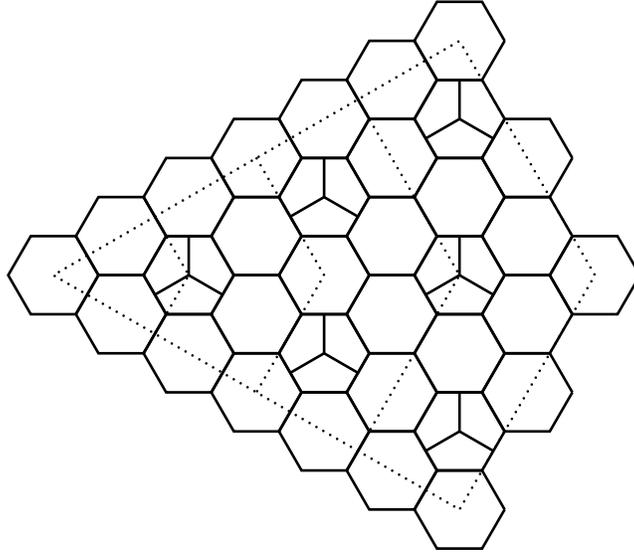
FIGURE 10. Fundamental domains for the $I(5,7)$-fulleroids $H_1$ to $H_4$ (dotted lines).

Infinitely many $I$-fulleroids can be obtained by applying the pentacon and triacon operations to the icosahedral fullerenes. In particular, the $P$ operation can be applied to any icosahedral fullerene except $G_{1,0}$ (the dodecahedron). The resulting fulleroid will be of type $(5, 6, 7)$ except for $G_{1,1} = C_{60}(I_h)$, $G_{2,0} = C_{80}(I_h)$ and $G_{2,1} = C_{140}(I)$, namely the three cases appearing in Table 2. In a similar way, either one of $T_1$ and $T_2$ or $T_3$ can be applied to any icosahedral fullerene, depending on whether the 3-fold rotational axes meet (hexagonal) faces or vertices, respectively. This gives rise to three additional infinite families of fulleroids, but again all except finitely many of these fulleroids will be of type $(5, 6, n)$ for some $n > 6$.

On the other hand, an infinite series of $I(5,7)$-fulleroids $(H_n)_{n>0}$ is obtained from the series $(G_{2n+1,0})_{n>0}$ by applying $T_1$ in a regular pattern to one fourth of all hexagons (instead of just to those hexagons which contain a 3-fold rotational axis). The pattern is shown in Figure 10 together with fundamental domains for the first four of these $I(5,7)$-fulleroids. The fundamental domains are kite-shaped pieces of different sizes from the modified hexagonal grid. The axes of the 5- and the 3-fold rotations will go through the leftmost and rightmost vertex, respectively, of the kite. Note that the first $I(5,7)$-fulleroid of this series, $H_1$, is just $F_{5,7}(I_h)$.

A similar series $(O_n)_{n>0}$ of $I(5,8)$-fulleroids is obtained from $(G_{2n+1,0})_{n>0}$ by applying $T_2$ instead of $T_1$ in the same pattern as shown in Figure 10.

## 4. Restrictions on the p-vectors

Let us first recall the well-known fact that, while the number of hexagons in a tiling with constant vertex degree 3 is arbitrary, the number of pentagons can be determined from the number of faces of degree 7 or larger. Indeed, the number of edges is $e = \frac{1}{2} \sum i \cdot p_i$, the number of vertices is $v = \frac{1}{3} \sum i \cdot p_i$, thus by Euler's

formula $f - e + v = 2$, we obtain

$$2 = \sum(1 - \frac{i}{2} + \frac{i}{3})p_i = \sum(1 - \frac{i}{6})p_i$$

or

(4.1) $$0 = 12 + \sum(i - 6)p_i.$$

For tilings with specified symmetries, much stronger conditions on the potential p-vectors are obtained by applying some elementary group theory. Let $T$ be some tiling of the sphere and let $G$ be a subgroup of its full symmetry group. First, note that the image of an arbitrary face of $T$ by an arbitrary element of $G$ is again a face of $T$. Therefore, $G$ can be interpreted as acting by permutations on the set of faces. By the same argument, $G$ also acts on the set of edges and on the set of vertices. Recall that the *stabilizer* of some element $x$ (i.e. some face, edge or vertex) is the set of operations in $G$ which map it onto itself. The stabilizer of $x$ is always a subgroup of $G$ and is denoted by $G_x$. The orbit $G \cdot x$ of an element $x$ is the set of images of $x$ under all the operations in $G$. Obviously, the set of orbits forms a partition of the set of elements, thus, for example, the set of all face orbits under $G$ forms a partition of the set of faces, and so on. The following elementary statement from group theory tells us how many elements these orbits can have.

LEMMA 4.1. *If $G$ is a finite group acting on a finite set $S$ and $s$ is an arbitrary element of $S$, then $\#(G \cdot x) = \#G/\#G_x$.*

Now, consider a tiling $T$ with symmetry group $I$, the group of orientation preserving symmetries of the icosahedron. All the elements of $I$ are rotations. If some rotation maps a face $f$ onto itself, then all the powers of this rotation do so, too. Moreover, no two rotations of different orders can fix the same face. Thus, the possible face stabilizers are exactly the groups generated by the rotations of orders 2, 3 and 5.

Another elementary fact is that the stabilizers of two elements in the same orbit are conjugate to each other, and that, moreover, if some subgroup $H$ of $G$ is conjugate to a stabilizer $G_x$, then $H$ is the stabilizer of some element in the same orbit as $x$. Now, since in $I$, each pair of rotational subgroups of the same order are conjugate, the following statement holds.

THEOREM 4.2. *In an $I$-fulleroid, there is at most one orbit of faces with rotational symmetries of orders 2, 3 and 5 respectively. These orbits, if existent, contain exactly 30, 20 and 12 faces, respectively. All the other orbits have trivial stabilizers and contain exactly 60 faces, each.*

Table 3 gives an overview of the possible combinations of face orbits.

| orbit size | 60 | 30 | 20 | 12 |
|---|---|---|---|---|
| number of orbits | any | $\leq 1$ | $\leq 1$ | 1 |
| face degree | any | 2t | 3t | 5t |

TABLE 3. The possible face orbits of an $I$-fulleroid.

Now, a rotation of order 2 can never fix a face or vertex of odd degree, So, in this case, it has to fix either an edge or a face of even degree. Similarly, a rotation of order 3 must fix either a vertex or a face of some degree divisible by 3. On the other

hand, a rotation of order 5 must fix a face, since there is no other element it could possibly fix. We can distinguish two broad classes of $I(5, n)$-fulleroids depending on whether or not the 5-fold rotations fix pentagons or larger faces. In the first case, the $p$-vector will be of the form

$$\mathbf{A}_{n,k} \colon (p_5, p_n) = \left( 12 + 60k, \frac{60k}{n-6} \right),$$

where $k \geq 1$, $n \geq 6$ and $p_n \in \mathbf{N}$. In the second case, it will be of the form

$$\mathbf{B}_{n,k} \colon (p_5, p_n) = \left( 60k, 12\frac{5k-1}{n-6} \right),$$

where $k \geq 1$, $n \geq 10$, $5|n$ and $p_n \in \mathbf{N}$. In the following, we will give a finer parametrization of potential $p$-vectors.

For a given degree $i$, let $m_i$ denote the number of orbits of $i$-faces (i.e. faces of degree $i$) that are not mapped onto themselves by any symmetry but the identity. The total number of such faces is then $60m_i$ by the above. For $j = 2, 3, 5$, set $k_j := k$, if a $k \cdot j$-face exists which is fixed by a rotation of order $j$. If none such face exists for any $k$, then we set $k_j := 6/j$.

LEMMA 4.3. *For each I-fulleroid, the equality*

$$\sum_i m_i(i-6) + \sum_{j=2,3,5} k_j = 6$$

*holds.*

PROOF. Each face orbit has either a trivial stabilizer or is fixed by a rotation of order 2, 3 or 5. If some face $f$ of degree $m$ has a stabilizer of order $j = 2, 3, 5$, then we have $m = k_j \cdot j$, and the orbit of $f$ contains exactly $60/j$ faces. Together with Equation 4.1, this implies

$$0 = \sum_i 60m_i(i-6) + \sum_{j=2,3,5} \frac{60}{j}(k_j \cdot j - 6) + 12.$$

Note that this equation remains true if for some $j$, there is no face fixed by a rotation of order $j$, because in that case we have $k_j = 6/j$, thus $k_j \cdot j - 6 = 0$.

We divide both sides by 60 and simplify the second sum, to obtain

$$
\begin{aligned}
0 &= \sum_i m_i(i-6) + \sum_{j=2,3,5} k_j - \sum_{j=2,3,5} \frac{6}{j} + \frac{1}{5} \\
&= \sum_i m_i(i-6) + \sum_{j=2,3,5} k_j - \frac{6}{2} - \frac{6}{3} - \frac{6}{5} + \frac{1}{5} \\
&= \sum_i m_i(i-6) + \sum_{j=2,3,5} k_j - 6.
\end{aligned}
$$

$\square$

We finish this section by giving formulae to calculate the p-vector and the number of vertices $v$ from the invariants $m_i$ and $k_j$. Since the invariants are insensitive to the number of hexagons, the following equations hold if and only if the fulleroid

in question does not contain hexagons. For the p-vector, we have

$$(4.2) \qquad p_i = 60 \cdot \left( m_i + \sum_{j \cdot k_j = i} \frac{1}{j} \right).$$

The number of vertices is

$$v = \frac{1}{3} \sum_i i \cdot p_i = 20 \cdot \sum_i \left( i \cdot m_i + \sum_{j \cdot k_j = i} \frac{i}{j} \right)$$

$$= 20 \cdot \sum_i \left( i \cdot m_i + \sum_{j \cdot k_j = i} k_j \right),$$

thus

$$(4.3) \qquad v = 20 \cdot \left( \sum_i i \cdot m_i + \sum_{j \cdot k_j \neq 6} k_j \right).$$

## 5. From the p-vectors to the structures

In the following, we will present a general method for the classification of $I$-fulleroids with given parameters $m_i$ and $k_j$. This method easily generalizes to other, similar problems. We will present proofs for the individual classification results at different levels of abstraction, starting with an elementary proof of the uniqueness of $F_{5,10}(I_h)$ and gradually transforming our arguments into purely combinatorial ones expressed in the language of Delaney symbols. Our intention is to demonstrate thereby how Delaney symbols capture the essential structural information in a very natural and convenient way.

PROPOSITION 5.1. *The fulleroid $F_{5,10}(I_h)$ is the only I-fulleroid with p-vector $(p_5, p_{10}) = (60, 12)$ and the smallest $I(5, 10)$-fulleroid.*

PROOF. First note that 12 is the smallest possible non-zero value of $p_{10}$, corresponding to the parameter values $m_{10} = 0$ and $k_5 = 2$. This means that there is exactly one orbit of decagons, each of which is fixed by a rotation of order 5, and one orbit of pentagons, which have trivial stabilizers. This gives us the additional information that all the rotation axes of order 2 meet edges and that all the axes of order 3 meet vertices. Let $v_0$ be one such vertex and let $f_0$ be one of the faces adjacent to it.

Assume $f_0$ is a decagon. Because of the 5-fold rotation mapping $f_0$ onto itself, every second vertex of $f_0$ must meet a 3-fold axis. The three faces containing such a vertex must then all be decagons, because they are rotated onto each other. This means that $f_0$ ist completely surrounded by decagons, each of them in the same orbit as $f_0$. By induction, all the faces in the connected component which contains $f_0$ are decagons. There is only one connected component, so there are only decagons, a contradiction.

We conclude that $v_0$ must be adjacent to a pentagon. Again, this implies that all three faces adjacent to $v_0$ are pentagons. Let $v_1$ be a vertex adjacent to any two of these faces. The third face adjacent to $v_1$ cannot be a pentagon, since this pentagon would be in the same orbit as $f_0$ and thus contain a symmetric image $v_2$ of $v_0$, i.e., a vertex meeting a 3-fold rotation axis. There are three essentially
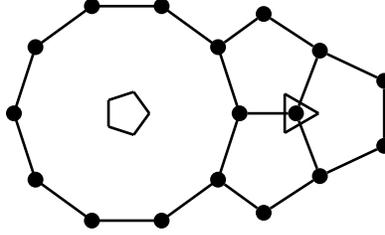
FIGURE 11. A forced subgraph for an $I$-fulleroid with p-vector
$(p_5, p_{10}) = (60, 12)$.

different possible positions for $v_2$. In each case, by applying all symmetries one
finds that the resulting structure must be the dodecahedron.

Consequently, the third face meeting $v_2$ is a decagon, thus the fulleroid in
question must contain the substructure depicted in Figure 11, where the 3- and the
5-fold rotation centers are indicated by a small triangle and pentagon, repectively.
By applying these rotations in a systematic way, one obtains the structure shown
in Figure 6.                                                                    □

Obviously, the argumentation in the above proof is straightforward but—with
all the details worked out—rather tedious. This is partly due to the fact that
instead of individual faces, edges and vertices, we have to deal with whole orbits,
taking all symmetries known so far into account. It is much more convenient to
work in the *orbit space* of the group $I$. The orbit space of some group $\Gamma$ is defined
as the image of a continous function which maps two points $p$ and $q$ of the sphere
onto the same image point if and only if there is some element of $\Gamma$ which maps $p$
to $q$. The orbit space of $I$ is, topologically, just a sphere with three special points,
namely the images of the three types of rotational centers. A simple way to obtain
the orbit space is to take a fundamental domain and glue together boundary points
which are mapped onto each other by some group element.

The degree of the image of a face in the orbit space depends on the stabilizer
of that face. In general, an $(i \cdot j)$-face with a rotation center of order $j$ is mapped
to an $i$-face. Likewise, vertices with non-trivial stabilizers are mapped to vertices
of accordingly smaller degree. Therefore, in the orbit space, we have to consider
special features like 1-gons and vertices of degree 1. Still more strangely, the image
of an edge with 2-fold stabilizer is a "half-edge" with only one endpoint. A loop
edge, one which has two identical endpoints, must be count twice when determining
the vertex degree. Likewise, an edge adjacent to the same face on both sides has
to be count twice when determining the face degree. In both cases, however, a
half-edge is only count once.

Despite these difficulties, we can simplify our arguments considerably by work-
ing in the orbit space. We will call the image of a tiling in the orbit space its *orbit
tiling*.

PROPOSITION 5.2. *The fulleroid* $F_{5,8}(I_h)$ *is the only $I$-fulleroid with p-vector*
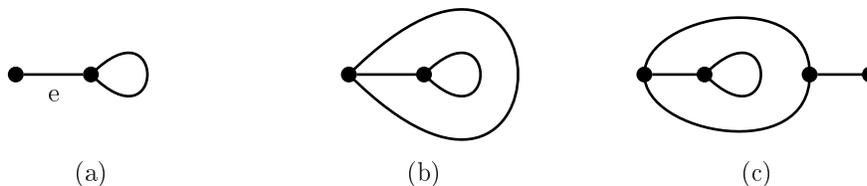$(p_5, p_8) = (72, 30)$ *and the smallest $I(5, 8)$-fulleroid.*

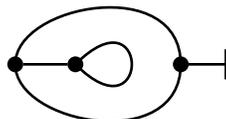FIGURE 12. Forced subgraphs for the smallest $I(5,8)$-fulleroid.



FIGURE 13. The orbit space of $F_{5,9}(I_h)$

PROOF. Again, $p_8 = 30$ is the smallest possible value of $p_8$, since 2 is the largest rotational order occuring in $I$ which divides 8. The p-vector $(p_5, p_8) = (72, 30)$ corresponds to the parameter values

$$(m_5, m_8, k_2, k_3, k_5) = (1, 0, 4, 2, 1).$$

The orbit tiling consists of a 1-gon (the image of a 5-fold symmetric pentagon), a 5-gon (the image of an asymmetric pentagon) and a 4-gon (the image of a 2-fold symmetric octagon). Exactly one degree 1 vertex and no half-edge occurs, because there are 2-fold symmetric, but no 3-fold symmetric faces.

The 1-gon gives rise to the subgraph depicted in Figure 12(a), because of the free valency at its vertex. The edge $e$ is adjacent to the same face at both sides, thus if that face is a 4-gon, then the configuration of Figure 12(b) occurs. Now, both vertices have degree 3, so there is no possible continuation. We conclude that the 1-gon must be adjacent to the pentagon, leading to the configuration of Figure 12(c).

Now, the outer face is a 4-gon and there is exactly one vertex of degree 1, as required. The configuration is unique, as shown, and corresponds to the $I$-fulleroid $F_{5,8}(I_h)$. □

PROPOSITION 5.3. *The fulleroid $F_{5,9}(I_h)$ is the only $I$-fulleroid with p-vector $(p_5, p_9) = (72, 20)$ and the smallest $I(5,9)$-fulleroid.*

PROOF. As above, $p_9 = 20$ is smallest possible and the parameter values follow uniquely from the p-vector. The orbit tiling consists of a 1-gon and a pentagon as above and a triangle corresponding to an orbit of 3-fold symmetric 9-gons. We have no vertex of degree 1, but a half-edge. As above, the 1-gon must be adjacent to the pentagon, which in turn must be adjacent to the triangle. The only possible configuration is shown in Figure 13, where the half-edge is shown as a "T-shape" (note that a half-edge counts only once, so the outer face is indeed a triangle). □

PROPOSITION 5.4. *The fulleroid $F_{5,12}(I_h)$ is the only $I$-fulleroid with p-vector $(p_5, p_{12}) = (192, 30)$ and the smallest $I(5,12)$-fulleroid.*

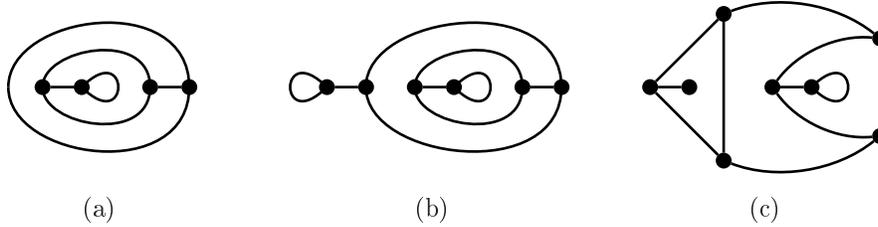(a)                          (b)                          (c)

FIGURE 14. Forced subgraphs referred to in Proposition 5.4.

PROOF. First, we must show that no *I*-fulleroid with the smaller p-vector $(p_5, p_{12}) = (132, 20)$ exists. For such a structure, the orbit tiling would contain a 1-gon, a quadrangle and two pentagon. As in the proof of proposition 5.2, the 1-gon must be adjacent to a pentagon $f_0$. The other face adjacent to $f_0$ cannot be the quadrangle, since that would lead to the configuration of Figure 12(c). On the other hand, if $f_0$ is adjacent to the second pentagon, the configuration of Figure 14(a) results, which cannot be continued by a quadrangle. Thus, we have no *I*-fulleroid with face-vector $(p_5, p_{12}) = (132, 20)$ and come to check the next possible p-vector $(p_5, p_{12}) = (192, 30)$.

Here, in the orbit space, we have a 1-gon, a hexagon (the image of the 2-fold symmetric 12-gon) and three pentagons. We have no half-edge, but a degree 1 vertex. We already know that if the 1-gon is adjacent to a pentagon $f_0$, then $f_0$ can not be adjacent to a second pentagon. Let us assume that $f_0$ is adjacent to the hexagon, which we will denote by $f_1$. Now, $f_1$ must be adjacent to a second pentagon, but has only one vertex with a free valency on its boundary. This enforces a configuration as in Figure 14(b), in contradiction to the fact that we must have a third pentagon.

We conclude that the 1-gon must be adjacent to the hexagon. Again, there is only one possible continuation, leading to the configuration in Figure 14(c), which is legal.                                                                    ☐

The reader is invited to proof the last 3 propositions in the straightforward manner of Proposition 5.1. Obviously, working in the orbit space simplifies things a lot. On the other hand, strange features like half-edges, loops and dead-end edges make the necessary case-analysis unintuitive and error-prone. Moreover, for more complicated tasks, the help of a computer will be indispensable. Therefore, a convenient combinatorial encoding which naturally includes all the singularities mentioned above should be most desirable. Such an encoding is provided by the Delaney symbol, as introduced by A. Dress [**Dre84**] and inspired by M. Delaney [**Del80**].

Delaney symbols habe been treated extensively in several publications (see for example [**DDMP93, DDH95**], and, of course, [**DB96**]). We will only give an informal introduction here. For a given tiling, connect the center of each face to each of its vertices by a dotted line and to the midpoint of each of its edges by a dashed line as in Figure 15.

The result is a triangulation called the *barycentric subdivision*. Each of its triangles has exactly one dotted, one dashed and one solid edge. The subdivision can be performed in such a way that it is invariant under the symmetry group of the tiling. Then, obviously, the stabilizer of each triangle is trivial. The image of
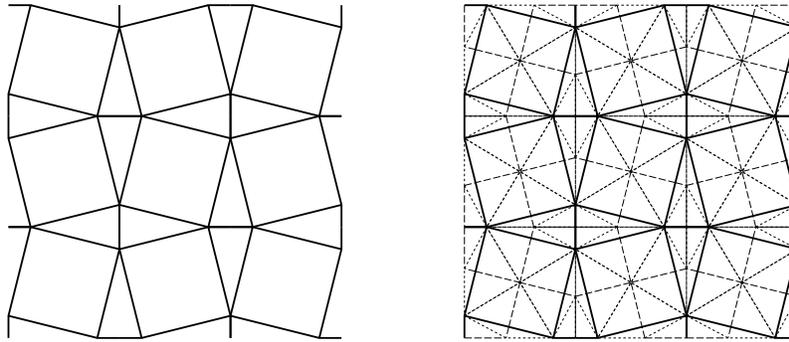
FIGURE 15. A tiling of the plane and its barycentric subdivision.

the barycentric subdivision in the orbit space is a subdivision of the orbit tiling into triangles such that again each triangle has exactly one dotted, one dashed and one solid edge. For example, the configuration of Figure 13 corresponds to the triangulation of the orbit space shown in Figure 16.
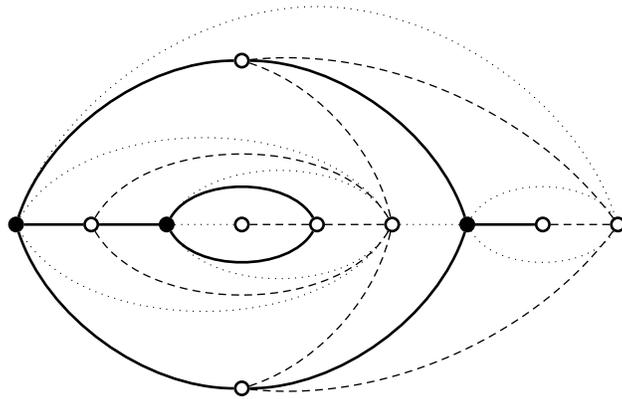


FIGURE 16. The barycentric triangulation of Figure 13.

Admittedly, this looks much more complicated than the original figure. It has, on the other hand, the advantage that the whole structure can be conveniently encoded by listing adjacent pairs of triangles sorted by the respective type (i.e. dotted, dashed or solid) of edge they are sharing. Since pairs of triangles can share more than one edge, a particular pair of triangles may occur more than once. A simple way to visualize the adjacency relations is to construct the dual graph of the orbit triangulation as in Figure 17. Here, to each triangle of Figure 16 (shown in gray), we assign a node, and we connect two nodes by a dotted, dashed or solid line, respectively, if the corresponding triangles share an edge of the same type. The resulting regularly edge-labelled graph is called the *Delaney graph* of the original tiling. The complete *Delaney symbol* is obtained by sublementing this graph with information on the images of the rotational axes. For details, see e.g. [**DDMP93**].

All we need to know in this context is how certain subgraphs of the Delaney graph correspond to the vertices, faces and edges of the orbit tiling. Note that
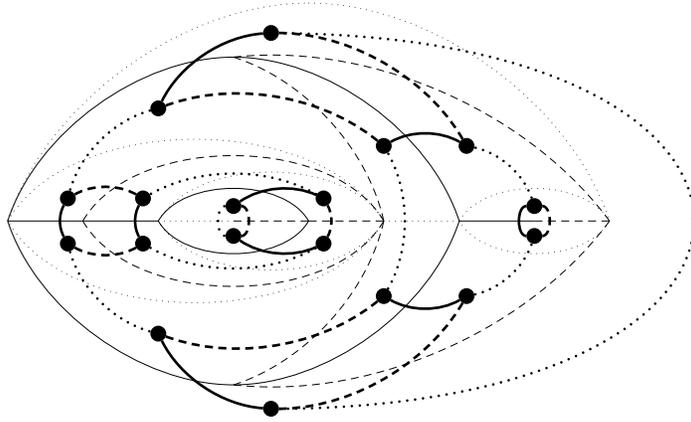
FIGURE 17. The triangulated orbit space (thin lines) and the De-
laney graph of $F_{5,9}(I_h)$.

if we remove all edges of a certain type, the remaining subgraph is a collection
of cycles (this is only true if the symmetry group of the original tiling does not
contain reflections). Each of these cycles corresponds to a constituent of the orbit
tiling. In particular, dotted-dashed cycles correspond to faces, dotted-solid cycles
to vertices and dashed-solid cycles to edges. The length of a dotted-dashed cycle
is twice the degree of the corresponding face. The length of a dotted-solid cycle is
twice the degree of the corresponding vertex. The length of a dashed-solid cycle is
four if that cycle corresponds to an ordinary edge and two if it corresponds to a
half-edge. An additional fact that helps to simplify the necessary case analysis is
that the Delaney graph of a tiling with orientation preserving symmetry group is
always *bipartite*, i.e. its nodes can be labelled by '+' and '-' in such a way that no
edge connects two nodes with the same label.

PROPOSITION 5.5. *The fulleroid $F_{5,15}(I_h)$ is the only I-fulleroid with p-vector*
$(p_5, p_{15}) = (120, 12)$ *and the smallest I(5, 15)-fulleroid.*

PROOF. Obviously, the *p*-vector is smallest possible and corresponds to the
parameter values given in Table 1. Thus, the orbit tiling consists of one triangle
corresponding to an orbit of 3-fold symmetric 15-gons, and two pentagons. In
effect, in the Delaney graph, we have one dotted-dashed cycle of length 6 and two
dotted-dashed cycles of length 10. Moreover, all dotted-solid cycles will have length
6 except for one of length 2 (corresponding to an orbit of 3-fold symmetric vertices).
All dashed-solid cycles will have length 4 except for one of length 2 (corresponding
to an orbit of 2-fold symmetric edges). Both nodes belonging to the small dotted-
solid cycle $\mathcal{V}$ are contained in the same dotted-dashed cycle $\mathcal{F}$. There are two cases
depending on the length of $\mathcal{F}$.

Let us first assume that $\mathcal{F}$ has length 6 (see Figure 18). Denote by $a$ the solid
edge in $\mathcal{V}$. The dashed-solid component to which $a$ belongs consists of four nodes
already, so it must be completed to a cycle by a solid edge $b$. Now, to make the
Delaney graph connected, the cycle $\mathcal{F}$ must be connected to one of the dotted-
dashed cycles of length 10 by a solid edge $c$. Again, to complete a dashed-solid
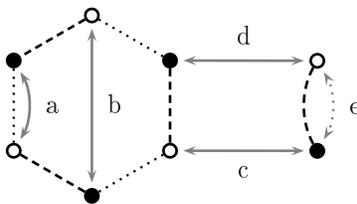cycle, a solid edge $d$ is forced. But now, $b$, $c$ and $d$ belong to a common dotted-solid

FIGURE 18. A forced partial Delaney graph.

component with already 6 nodes, which has to be completed by a dotted edge $e$. This will produce a dotted-dashed cycle of length 2, which can not occur. The situation is depicted in Figure 18. We conclude that $\mathcal{F}$ can not have length 6.

Now let us assume that $\mathcal{F}$ has length 10. Again, denote by $a$ the solid edge in $\mathcal{V}$. Again, a solid edge $b$ is forced to complete a dashed-solid cycle. Let $r$ be the dotted neighbour of one of the nodes incident to $b$. By considering legal lengths of dotted-solid and dashed-solid cycles again, it can be seen easily that $r$ can not be connected by a solid line to any other node in $\mathcal{F}$. Therefore, $r$ must be connected by an edge $c$ to a different dotted-dashed cycle $\mathcal{G}$. We know that the length of $\mathcal{G}$ is at least 6, so we draw $\mathcal{G}$ as an incomplete cycle of length 6 in Figure 19. The solid edges $d$, $e$ and $f$ in this picture are forced by completion of a dashed-solid cycle, a dotted-solid cycle and a dashed-solid cycle, respectively.

The two remaining vertices of $\mathcal{F}$ can not be connected to each other by a solid edge, because this would lead to a dotted-solid cycle of length at least 8. Thus, there are edges $g$ and $h$ as in the picture connecting $\mathcal{F}$ to a dotted-dashed cycle $\mathcal{H}$, of which we don't know yet whether it is the same one as $\mathcal{G}$ or not. We only draw a portion of $\mathcal{H}$ containing 4 nodes. The solid edges $i$ and $j$ are enforced by the completion of dotted-solid cycles. Now, if $\mathcal{G}$ has only length 6, i.e. if the dashed edge $k$ is present, then the dashed edge $l$ is forced, thus $\mathcal{H}$ would have length 4, which is too short. If, on the other hand, $\mathcal{H}$ is equal to $\mathcal{G}$, then no connection to the third dotted-dashed cycle is possible. We conclude that $\mathcal{H}$ is different from $\mathcal{G}$ and has length 6, while $\mathcal{G}$ has length 10. This enforces edges $k$, $l$ and $m$ of Figure 20, which complete the Delaney graph. Obviously, this graph is legal (it contains, for example, exactly one dashed-solid cycle of length 2, as required), and our discussion above shows that it is unique.  □

For $F_{5,14}(I_h)$, the uniqueness proof is rather lengthy, so we will not present it here, but still manageable without computer support.

## References

[Cox71]   H.M.S. Coxeter. Virus macromolecules and geodesic domes. In J.C. Butcher, editor, *A selection of mathematics*. Auckland University Press, 1971.

[DB96]    A.W.M. Dress and G. Brinkmann. Phantasmagorical fulleroids. *Match*, 33:87–100, 1996.

[DDH95]   O. Delgado Friedrichs, A.W.M. Dress, and D.H. Huson. Tilings and symbols — a report on the uses of symbolic calculation in tiling theory. In J. Fleischer, J. Grabmeier, F.W. Hehl, and W. K"uchlin, editors, *Computer algebra in science and engineering*, pages 273–286. World Scientific, London, 1995.
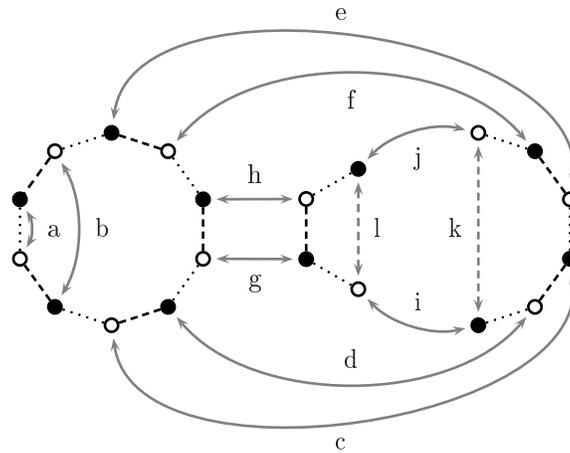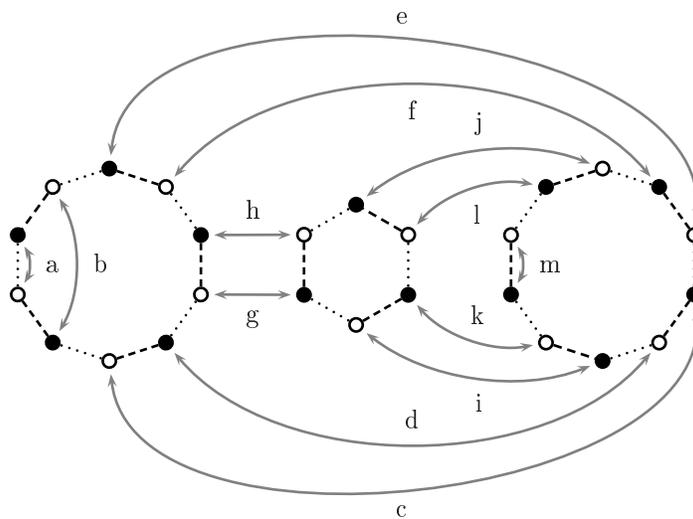
FIGURE 19. Another forced partial Delaney graph.



FIGURE 20. The Delaney graph of $F_{5,15}(I_h)$.

[DDMP93]  O. Delgado Friedrichs, A.W.M. Dress, A. Müller, and M.T. Pope. Polyoxometalates:
          A class of compounds with remarkable topology. *Molecular Engineering*, 3:9–28, 1993.
[Del80]   M.S. Delaney. Quasisymmetries of space group orbits. *Match*, 9:73–80, 1980.
[Del98]   O. Delgado Friedrichs. Fast and simple embeddings of planar graphs. to appear in:
          *Proceedings of the Dimacs Workshop on Discrete Mathematical Chemistry*, 1998.
[DG97]    M. Deza and V.P. Grishukhin. Face-regular bifaced polyhedra. Preprint LIENS 97-10,
          Ecole Normale Superieure, Paris, 1997.
[Dre84]   A.W.M. Dress. Regular polytopes and equivariant tessellations from a combinatorial
          point of view. In *Algebraic Topology*, pages 56–72. SLN 1172, Göttingen, 1984.
[Gol37]   M. Goldberg. A class of multisymmetric polyhedra. *Tohoku Mathematical Journal*,
          43:104–108, 1937.
[Grü67]   B. Grünbaum. *Convex Polytopes*. John Wiley & Sons, Ltd., London,New York,Sydney,
          1967.

[Hus93]    D.H. Huson. The generation and classification of tile-$k$-transitive tilings of the euclidean plane, the sphere and the hyperbolic plane. *Geometriae Dedicata*, 47:269–296, 1993.

OLAF DELGADO FRIEDRICHS, FAKULTÄT FÜR MATHEMATIK, UNIVERSITÄT BIELEFELD, 33501 BIELEFELD, GERMANY.
    *E-mail address*: `delgado@Mathematik.Uni-Bielefeld.DE`

MICHEL DEZA, DMI-LIENS, ECOLE NORMALE SUPERIEURE, 45 RUE D'ULM, 75005, PARIS, FRANCE.
    *E-mail address*: `deza@dmi.ens.fr`